JST: Smart Systems and Devices
Volume 34, Issue 2, May 2024, 066-074

Adaptive Fast Terminal Sliding Mode Control for Inverted Pendulum on Cart

Thi-Van-Anh Nguyen, Xuan-Hiep Nguyen, Quy-Thinh Dao*
Hanoi University of Science and Technology, Ha Noi, Vietnam
** Corresponding author email: thinh.daoquy@hust.edu.vn*

Abstract

This paper presents an innovative control strategy, the Adaptive Fast Terminal Sliding Mode Control (AFTSMC), designed for the stability control of an inverted pendulum on a cart. The proposed controller aims to stabilize the system within a finite time, leveraging the advantages of fast terminal sliding mode techniques. The system's dynamic model is employed to derive the controller, utilizing an adaptive approach to accommodate uncertainties and disturbances. Simulations are conducted to validate the proposed AFTSMC, comparing its performance with an Adaptive Sliding Mode Controller under various scenarios. The results demonstrate the efficacy of the AFTSMC in achieving stable and precise control, making it a promising solution for the challenging dynamics of inverted pendulum systems.

Keywords: Sliding mode control, adaptive fast terminal sliding mode control, inverted pendulum.

1. Introduction

The control of an inverted pendulum on a cart presents two essential objectives: swing-up and stability control. The swing-up task involves transitioning the pendulum from hanging to upright, while stability control concerns maintaining this delicate equilibrium. Achieving both objectives demands robust control strategies capable of addressing such systems' inherent instability and nonlinear dynamics.

In addressing swing-up control, energy-based strategies leverage the system's energy dynamics to facilitate a controlled transition to the upright position. Methods such as Energy Shaping [1-3], Passivity-Based Control [4, 5], and Optimal Control Approaches [6, 7] offer solutions tailored for managing the pendulum's energy distribution.

In the pursuit of stability control, various methodologies have been explored. Proportional-Integral-Derivative (PID) control [8-10], known for its simplicity and widespread application, is often used to stabilize systems. However, its effectiveness in handling highly nonlinear and uncertain systems might be limited.

Another approach, Linear Quadratic Regulator (LQR) control, aims to optimize system performance by defining a cost function [10-12]. While offering excellent performance under ideal conditions, LQR is highly reliant on an accurate system model, making it sensitive to model inaccuracies and variations.

Another option for stability control of an inverted pendulum is Model Predictive Control (MPC), a methodology that anticipates future system behaviour and manages constraints [13-15]. However, its implementation demands substantial computational resources and relies heavily on accurate modelling, posing challenges for real-time applications.

Sliding Mode Control (SMC) is another significant approach for stability control in an inverted pendulum system [16-20]. This control strategy, known for its robustness against uncertainties and disturbances, presents a compelling solution for stabilizing such inherently unstable systems. In the context of an inverted pendulum, SMC employs a sliding surface to guide the system state, ensuring stability even in the presence of uncertainties or external disturbances. Its inherent robustness allows the system to maintain stability by switching control actions, directing the system state towards the defined sliding surface. This characteristic makes SMC particularly effective for systems prone to unpredictable disturbances, a common trait in inverted pendulum configurations.

Emphasizing stability control and leveraging the inherent benefits of SMC, this paper presents a pioneering method—the Adaptive Fast Terminal Sliding Mode Control (AFTSMC). AFTSMC is specifically tailored to address stability concerns in inverted pendulum-cart systems. Integrating adaptive mechanisms with fast terminal sliding mode techniques, the proposed AFTSMC aims to enhance the robustness of SMC by incorporating adaptability, allowing

ISSN 2734-9373
https://doi.org/10.51316/jst.174.ssad.2024.34.2.8
Received: Mar 7, 2024; revised: Mar 18, 2024;
accepted: Mar 18, 2024

real-time adjustments in control parameters to counteract varying system dynamics or uncertainties.

The proposed AFTSMC primarily emphasizes stability control, aiming to maintain the pendulum in an upright position on the cart. While the swing-up task remains pivotal for the inverted pendulum system, the paper primarily focuses on the stability control aspect. The discussion on swing-up serves as a contextual foundation, recognizing its importance in the broader context of controlling inverted pendulum systems.

The development of AFTSMC strives to combine the robustness of SMC with adaptive mechanisms, creating a more effective and versatile stability control strategy for inverted pendulum systems. The proposed AFTSMC approach is anticipated to exhibit superior performance in maintaining stability within simulated environments compared to traditional SMC-based approaches.

The paper initiates with the following sections detailing: the modelling of the inverted pendulum on a cart in Section 2, the development of the adaptive fast terminal sliding mode control in Section 3, presentation of simulation results in Section 4, and concludes with a summary and key finding in Section 5.

2. Modelling of the Inverted Pendulum on a Cart

The configuration of the inverted pendulum on a cart, illustrated in Fig. 1, involves a pendulum affixed to a cart. Within this setup, m_p (kg) denotes the mass of the pendulum, and m_c (kg) represents the mass of the cart. The length of the pendulum is symbolized as l (m), where θ characterizes the pendulum's rotational angle from the y-axis in radians. The force applied to the cart along the x-axis is denoted by u, and g designates the gravitational acceleration vector.

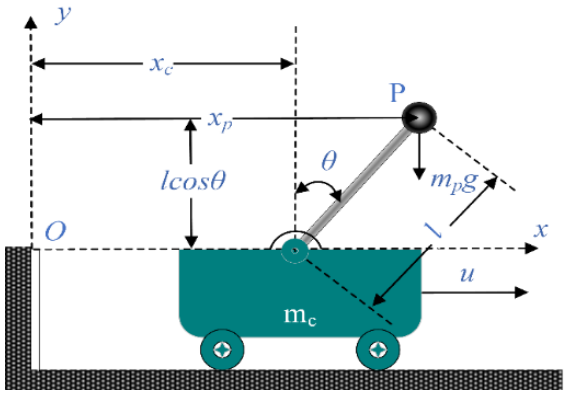

Fig. 1. Schematic of the inverted pendulum on a cart system.

The coordinates of the pendulum's center, denoted as (x_p, y_p) are determined as follows:

$$\begin{cases} x_p = x_c + l\sin\theta \\ y_p = l\cos\theta \end{cases} \tag{1}$$

where x_c is the cart position.

The speed of the pendulum:

$$\begin{cases} \dot{x}_p = \dot{x}_c + l\dot{\theta}\cos\theta \\ \dot{y}_p = -l\dot{\theta}\sin\theta \end{cases} \tag{2}$$

The kinetic energy of the pendulum is expressed as:

$$\begin{aligned} T_p &= \frac{1}{2}m_p\dot{x}_p^{\,2} + \frac{1}{2}m_p\dot{y}_p^{\,2} + \frac{1}{2}J\dot{\theta}^2 \\ &= \frac{1}{2}m_p\dot{x}_c^{\,2} + m_p l\dot{x}_c\dot{\theta}\cos\theta \\ &\quad + \frac{1}{2}(J + m_p l^2)\dot{\theta}^2 \end{aligned} \tag{3}$$

where $J = \frac{1}{3}m_p l^2$ is the equivalent moment of the pendulum.

The kinetic energy of the cart is:

$$T_c = \frac{1}{2}m_c\dot{x}_c^{\,2} \tag{4}$$

Combining (3) and (4), the total kinetic energy of the system is given by:

$$\begin{aligned} T = T_p + T_c &= \frac{1}{2}(m_c + m_p)\dot{x}_c^{\,2} \\ &\quad + m_p l\dot{x}_c\dot{\theta}\cos\theta + \frac{1}{2}(J + m_p l^2)\dot{\theta}^2 \end{aligned} \tag{5}$$

Since the cart moves horizontally, its potential energy remains constant. The potential energy of the system is solely attributed to the pendulum:

$$V = m_p g y_p = m_p g l\cos\theta \tag{6}$$

From (5) and (6), the Lagrangian of the system can be obtained as follows:

$$\begin{aligned} L = T - V &= \frac{1}{2}(m_c + m_p)\dot{x}_c^{\,2} + m_p l\dot{x}_c\dot{\theta}\cos\theta \\ &\quad + \frac{1}{2}(J + m_p l^2)\dot{\theta}^2 - m_p g l\cos\theta \end{aligned} \tag{7}$$

The motion equation of the system is given by:

$$\frac{d}{dt}\left(\frac{\delta L}{\delta \dot{q}_i}\right) - \frac{\delta L}{\delta q_i} = Q_i \tag{8}$$

where Q_i is the generalized force, the variables q_i are called generalized coordinates. For the pendulum, we define:

$$q^T = [x_c; \theta] \tag{9}$$

The corresponding velocities are:

$$\dot{q}^T = [\dot{x}_c; \dot{\theta}] \tag{10}$$

Equation (8) becomes:

$$\begin{cases} \dfrac{d}{dt}\left(\dfrac{\delta L}{\delta \dot{x}_c}\right) - \dfrac{\delta L}{\delta x_c} = u \\ \dfrac{d}{dt}\left(\dfrac{\delta L}{\delta \dot{\theta}}\right) - \dfrac{\delta L}{\delta \theta} = 0 \end{cases} \tag{11}$$

We have

$$\begin{cases} (m_c + m_p)\ddot{x}_c + m_p l\ddot{\theta}\cos\theta - m_p l\dot{\theta}^2 \sin\theta = u \\ m_p l\ddot{x}_c \cos\theta + (J + m_p l^2)\ddot{\theta} - m_p gl \sin\theta = 0 \end{cases} \tag{12}$$

As a result, the dynamic behaviour of the pendulum can be described by the following equation:

$$\ddot{\theta} = \frac{(m_c + m_p)g\sin\theta - m_p l\dot{\theta}^2 \sin\theta\cos\theta + u\cos\theta}{l\left[\dfrac{4}{3}(m_c + m_p) - m_p \cos^2\theta\right]} \tag{13}$$

Defining the state variable $x = [x_1; x_2]^T$ with $x_1 = \theta$ and $x_2 = \dot{\theta}$, (13) can be expressed as:

$$\begin{cases} \dot{x}_1 = x_2 \\ \dot{x}_2 = f(x) + g(x)u \end{cases} \tag{14}$$

where

$$f(x) = \frac{(m_c + m_p)g\sin x_1 - m_p l\dot{x}_2{}^2 \sin x_1 \cos x_1}{l\left[\dfrac{4}{3}(m_c + m_p) - m_p \cos^2 x_1\right]} \tag{15}$$

$$g(x) = \frac{\cos x_1}{l\left[\dfrac{4}{3}(m_c + m_p) - m_p \cos^2 x_1\right]} \tag{16}$$

After formulating the mathematical model of the pendulum system, the subsequent section will focus on designing control strategies for the system. This discussion will explore various methodologies to enhance stability and performance, involving controller synthesis and simulation results to evaluate their effectiveness.

3. Control Design

3.1. Fast Terminal Sliding Surface

The fundamental terminal sliding mode (TSM) surface is defined as:

$$s = \dot{x}_1 + \beta x_1^{\frac{q}{p}} = 0 \tag{17}$$

where $x_1 \in R$ represents the state, $\beta > 0$, and q, p $(q < p)$ are positive odd integers.

It can be readily demonstrated that, for an initial state $x_1(0) \neq 0$, when $s = 0$, the dynamics (17) will converge to $x_1 = 0$ in finite time:

$$t_s = \frac{p}{\beta(p-q)} |\, x_1(0)\,|^{\frac{p-q}{p}} \tag{18}$$

The equilibrium at $x_1 = 0$ is identified as a terminal attractor, signifying that the state $x_1 = 0$ can be reached in a stable manner within a finite time. The tuning of the parameters p, q, β allows for adjustment of the reaching time t_s.

The inclusion of the nonlinear term $\beta x_1^{q/p}$ is aimed at enhancing the convergent velocity and improving the convergence towards equilibrium. Closer proximity to equilibrium results in a faster convergence rate, leading to finite-time convergence. However, when the system state is significantly distant from equilibrium, the convergent velocity of the basic TSM surface (17) tends to be slower than that of the linear counterpart (achieved by setting $p = q$). This is because the term $x_1^{q/p}$ works to diminish the magnitude of the convergence rate at a distance from equilibrium. Consequently, to amplify the convergence rate of the basic TSM surface, the fast terminal sliding mode (FTSM) surface was introduced.

The fast terminal sliding mode (FTSM) surface is defined as:

$$s = \dot{x}_1 + \alpha x_1 + \beta x_1^{\frac{q}{p}} = 0 \tag{19}$$

where $x_1 \in R$, $\alpha, \beta > 0$, and q, p $(q < p)$ are positive integers.

The initial state $x_1(0) \neq 0$ reaching $x_1 = 0$ within the time interval is given by:

$$t_s = \frac{p}{\alpha(p-q)} \ln \frac{\alpha x_1(0)^{\frac{q-p}{p}} + \beta}{\beta} \tag{20}$$

By appropriately designing α, β, p, q the system state can achieve the equilibrium point in a finite time t_s. This is evident from (20), where:

$$\dot{x}_1 = -\alpha x - \beta x^{\frac{q}{p}} \tag{21}$$

The convergence time of the state x_1 is determined by the linear term $\dot{x}_1 = -\alpha x$ when x_1 is distant from the equilibrium point. Nevertheless, when the state x_1 approaches the origin $x_1 = 0$, the convergence time is dictated by the nonlinear term $\dot{x}_1 = -\beta x^{q/p}$. This results in exponential convergence of x to zero. The incorporation of the terminal attractor in the sliding surface (20) guarantees that the state converges to zero within a finite time.

Furthermore, the convergent velocity is assured when the state is far from the equilibrium 0. Consequently, the state can rapidly and precisely converge to equilibrium.

In this study, the control objective is to track the reference angle θ of the pendulum. The tracking error is defined as:

$$e = \theta - \theta_d \tag{22}$$

where θ is the angle of the pendulum, and θ_d is the reference angle. Consequently, the fast terminal sliding mode surface is expressed as:

$$s = \dot{e} + \alpha e + \beta e^{\frac{q}{p}} = 0 \tag{23}$$

3.2. Adaptive Fast Terminal Sliding Mode Controller

Within this section, we develop an adaptive fast terminal sliding mode controller for the inverted pendulum-cart system. To facilitate the controller design for the system (12) and assume that x_1 belong to the set which satisfy $\cos x_1 \neq 0$, we arrange (12) as follows:

$$\begin{cases} l\left[\frac{4}{3}(m_c+m_p) - m_p\cos^2 x_1\right]\dot{x}_2 = \\ \quad g\sin x_1(m_c+m_p) - mlx_2{}^2\cos x_1\sin x_1 + \cos x_2 u \\ l\left[\frac{4}{3}(m_c+m_p)\frac{1}{\cos x_1} - m_p\cos x_1\right]\dot{x}_2 = \\ \quad g\tan x_1(m_c+m_p) - mlx_2{}^2\sin x_1 + \end{cases} \tag{24}$$

Since $J = \frac{1}{3}m_p l^2$, then $\frac{4}{3}l = \frac{J+m_p l^2}{m_p l}$, and we have:

$$\left[\frac{J+m_p l^2}{m_p l}(m_c+m_p)\frac{1}{\cos x_1} - m_p l\cos x_1\right]\dot{x}_2 = g\tan x_1(m_c+m_p) - m_p lx_2{}^2\sin x_1 + \tag{25}$$

To create a controller without requiring model information, we opted for:

$$\begin{cases} \phi_1 = (m_c+m_p)\frac{J+m_p l^2}{m_p l}, \\ \phi_2 = (m_c+m_p)g, \\ \phi_3 = m_p l \end{cases}$$

as the unknown parameters of the system.

Considering outer disturbance, we transfer (16) to state-space form as:

$$\begin{cases} \dot{x}_1 = x_2 \\ g(x_1)\dot{x}_2 = u + \phi_2\tan x_1 - \phi_3 x_2{}^2\sin x_1 - dt \end{cases} \tag{26}$$

where $g(x_1) = \phi_1\frac{1}{\cos x_1} - \phi_3\cos x_1$, dt is the outer disturbance.

Based on a sliding mode function (23), the Lyapunov function is chosen as:

$$V = \frac{1}{2}g(x_1)s^2 + \frac{1}{2\gamma_1}(\phi_1-\hat{\phi}_1)^2 + \frac{1}{2\gamma_2}(\phi_2-\hat{\phi}_2)^2 + \frac{1}{2\gamma_3}(\phi_3-\hat{\phi}_3)^2 \tag{27}$$

where $\gamma_i > 0$, $\hat{\phi}_i$ is the estimation of ϕ_i $(i = 1,2,3)$.

Define two Lyapunov components as

$$\begin{cases} V_1 = \frac{1}{2}g(x_1)s^2 \\ V_2 = \frac{1}{2\gamma_1}(\phi_1-\hat{\phi}_1)^2 \\ \quad + \frac{1}{2\gamma_2}(\phi_2-\hat{\phi}_2)^2 + \frac{1}{2\gamma_3}(\phi_3-\hat{\phi}_3)^2 \end{cases} \tag{28}$$

Derivative of both sides of (28), we have:

$$\begin{cases} \dot{V}_1 = \frac{1}{2}\dot{g}(x_1)s^2 + g(x_1)s\dot{s} \\ \dot{V}_2 = -\frac{1}{\gamma_1}(\phi_1-\hat{\phi}_1)\dot{\hat{\phi}}_1 \\ \quad -\frac{1}{\gamma_2}(\phi_2-\hat{\phi}_2)\dot{\hat{\phi}}_2 - \frac{1}{\gamma_3}(\phi_3-\hat{\phi}_3)\dot{\hat{\phi}}_3 \end{cases} \tag{29}$$

From (26) we have

$$\dot{g}(x_1) = \left(\phi_1\frac{1}{\cos x_1}\tan x_1 + \phi_3\sin x_1\right)x_2 \tag{30}$$

We also obtain the derivative of the sliding surface s from (23) as

$$\begin{aligned} \dot{s} &= \ddot{e} + \alpha\dot{e} + \beta\frac{q}{p}e^{\frac{q}{p}-1}\dot{e} \\ &= (\dot{x}_2 - \ddot{\theta}_d) + \alpha\dot{e} + \beta\frac{q}{p}e^{\frac{q}{p}-1}\dot{e} \end{aligned} \tag{31}$$

Finally, we get

$$\begin{aligned} \dot{V}_1 = \phi_1\Bigg[&\frac{\tan x_1}{2\cos x_1}x_2 s^2 + \frac{1}{\cos x_1}s\left(\alpha\dot{e} + \beta\frac{q}{p}e^{\frac{q}{p}-1}\dot{e} - \ddot{\theta}_d\right) \\ &+ \phi_2 s\tan x_1 + \phi_3\Bigg[x_2 s\sin x_1\left(\frac{1}{2}s - x_2\right) \\ &- s\cos x_1\left(\alpha\dot{e} + \beta\frac{q}{p}e^{\frac{q}{p}-1}\dot{e} - \ddot{\theta}_d\right)\Bigg] + s(u - dt) \end{aligned} \tag{32}$$

The control law is defined as:

$$u = -\eta sgn(s) - \hat{\phi}_1\left[\frac{\tan x_1}{2\cos x_1}x_2 s + \frac{1}{\cos x_1}s\left(\alpha\dot{e} + \beta\frac{q}{p}e^{\frac{q}{p}-1}\dot{e} - \ddot{\theta}_d\right)\right] - \hat{\phi}_2\tan x_1 - \hat{\phi}_3\left[x_2\sin x_1\left(\frac{1}{2}s - x_2\right) - \cos x_1\left(\alpha\dot{e} + \beta\frac{q}{p}e^{\frac{q}{p}-1}\dot{e} - \ddot{\theta}_d\right)\right] \quad (33)$$

where η is a constant and $\eta \geq max|dt|$.

Applying the control law (33) to $\dot{V}_1$, we have

$$\dot{V}_1 = -\eta|s| - sdt + (\phi_1 - \hat{\phi}_1)\left[\frac{\tan x_1}{2\cos x_1}x_2 s^2 + \frac{1}{\cos x_1}s\left(\alpha\dot{e} + \beta\frac{q}{p}e^{\frac{q}{p}-1}\dot{e} - \ddot{\theta}_d\right)\right] + (\phi_2 - \hat{\phi}_2)s\tan x_1 + (\phi_3 - \hat{\phi}_3)\left[x_2 s\sin x_1\left(\frac{1}{2}s - x_2\right) - s\cos x_1\left(\alpha\dot{e} + \beta\frac{q}{p}e^{\frac{q}{p}-1}\dot{e} - \ddot{\theta}_d\right)\right] \quad (34)$$

From (29) and (34) we obtain

$$\begin{aligned}\dot{V} &= \dot{V}_1 + \dot{V}_2 \\ &= -\eta|s| - sdt \\ &+ (\phi_1 - \hat{\phi}_1)\left[\frac{\tan x_1}{2\cos x_1}x_2 s^2 + \frac{1}{\cos x_1}s\left(\alpha\dot{e} + \beta\frac{q}{p}e^{\frac{q}{p}-1}\dot{e} - \ddot{\theta}_d\right) - \frac{1}{\gamma_1}\dot{\hat{\phi}}_1\right] \\ &+ (\phi_2 - \hat{\phi}_2)(s\tan x_1 - \frac{1}{\gamma_2}\dot{\hat{\phi}}_2) \\ &+ (\phi_3 - \hat{\phi}_3)\left[x_2 s\sin x_1\left(\frac{1}{2}s - x_2\right) - s\cos x_1\left(\alpha\dot{e} + \beta\frac{q}{p}e^{\frac{q}{p}-1}\dot{e} - \ddot{\theta}_d\right) - \frac{1}{\gamma_3}\dot{\hat{\phi}}_3\right]\end{aligned} \quad (35)$$

The adaptive law is designed as follows:

$$\begin{cases}\dot{\hat{\phi}}_1 = \gamma_1\left[\frac{\tan x_1}{2\cos x_1}x_2 s^2 + \frac{1}{\cos x_1}s\left(\alpha\dot{e} + \beta\frac{q}{p}e^{\frac{q}{p}-1}\dot{e} - \ddot{\theta}_d\right)\right] \\ \dot{\hat{\phi}}_2 = \gamma_2 s\tan x_1 \\ \dot{\hat{\phi}}_3 = \gamma_3\left[x_2 s\sin x_1\left(\frac{1}{2}s - x_2\right) - s\cos x_1\left(\alpha\dot{e} + \beta\frac{q}{p}e^{\frac{q}{p}-1}\dot{e} - \ddot{\theta}_d\right)\right]\end{cases} \quad (36)$$

As a result, $\dot{V} = -\eta|s| - sdt < 0$.

This implies the stability of the system.

4. Simulation Results

In this section, some simulation scenarios are carried out to verify the effectiveness of the proposed controller in terms of the stability of the pendulum and control the pendulum to track desired trajectories. The pendulum parameters on a cart system are selected from the report of [21]. The mass of the cart is $m_c = 0.5kg$, the half-length of the pendulum is $l = 0.3m$, and gravitational acceleration is $g = 9.81\ (\mathrm{m/s^2})$.

4.1. Stable Control

To assess the stability capabilities of the proposed controller, the pendulum is stabilized to an upright position from various initialized angles. An Adaptive Sliding Mode Controller (ASMC) is selected as a counterpart to the proposed controller for comparative analysis. The control signal of ASMC controller is:

$$u = -\eta sgn(s) - \hat{\phi}_1\left(\frac{\tan x_1}{2\cos x_1}x_2 s + \frac{\alpha\dot{e} - \ddot{\theta}_d}{\cos x_1}\right) - \hat{\phi}_2\tan x_1 - \hat{\phi}_3\left[x_2\sin x_1\left(\frac{1}{2}s - x_2\right) - \cos x_1\left(\alpha\dot{e} - \ddot{\theta}_d\right)\right] \quad (37)$$

with an adaptive law

$$\begin{cases}\dot{\hat{\phi}}_1 = \gamma_1\left[\frac{\tan x_1}{2\cos x_1}x_2 s^2 + \frac{1}{\cos x_1}s\left(\alpha\dot{e} - \ddot{\theta}_d\right)\right] \\ \dot{\hat{\phi}}_2 = \gamma_2 s\tan x_1 \\ \dot{\hat{\phi}}_3 = \gamma_3\left[x_2 s\sin x_1\left(\frac{1}{2}s - x_2\right) - s\cos x_1\left(\alpha\dot{e} - \ddot{\theta}_d\right)\right]\end{cases} \quad (38)$$

Two criteria for evaluating the control performance are settling time and root mean square error (RMSE). The simulation results are succinctly presented in Table 1.

Table 1. Quantitative evaluation of stability simulation.

θ_0 (rad)		Settling time (s)		RMSE (rad)	
		FTSMC	SMC	FTSMC	SMC
Without noise	$\pi/15$	1.0	_	0.024	_
	$\pi/20$	1.0	3.2	0.012	0.027
	$\pi/25$	0.8	1.8	0.008	0.014
With noise	$\pi/15$	1.0	_	0.024	_
	$\pi/20$	1.0	3.8	0.012	0.027
	$\pi/25$	0.8	2.1	0.010	0.017

Notes: "-" means the controller cannot stabilize the pendulum.

Notably, the proposed controller consistently outperforms its counterpart across both evaluation criteria. For instance, with an initial angle of $\pi/25$ radians, the system under the proposed controller achieves stability after 0.8 seconds, compared to 1.8 seconds under the ASMC. Even at an initial angle of $\pi/15$, the AFTSMC effectively stabilizes the pendulum, whereas the ASMC struggles to maintain stability. Fig. 2 visually depicts the pendulum angles (θ) for both controllers in the stability control scenario, providing additional insights into their comparative performance.

In the upper subFig. of Fig. 2, the black line represents the reference signal, while the dashed blue and red lines depict the simulated angles controlled by the AFTSMC and ASMC controllers, respectively.

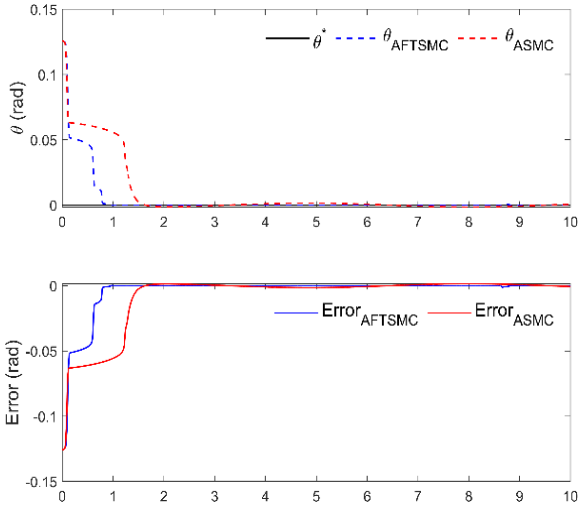

Fig. 2. The stability evaluation of two controllers when the pendulum's initial angle $\theta_0 = \pi/25$.

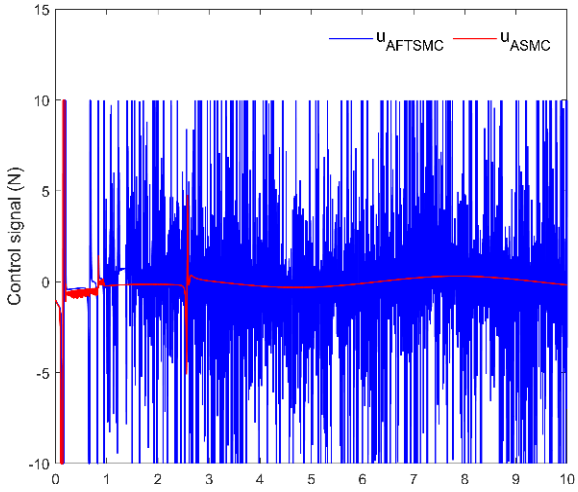

Fig. 3. The control signals of two controllers when stabilizing the pendulum from the initial angle $\theta_0 = \pi/25$.

Furthermore, both controllers exhibit the chattering phenomenon in the control signal, as observed in Fig. 3. This issue may have implications for actuator damage and a reduction in their operational lifespan.

To evaluate the robustness of the proposed controller, a random noise with a bandwidth of 1.0 N is introduced into the system as an external disturbance. As illustrated in Fig. 4, the Fast Terminal Controller adeptly addresses the external disturbance, exhibiting negligible impact on both settling time and Root Mean Square Error (RMSE) criteria. In contrast, the ASMC controller struggles to contend with the external disturbance, resulting in an RMSE that is ten times greater than when the disturbance is absent.

4.2. Tracking Control

In this subsection, the proposed controller's and its counterpart's performance is assessed while tracking a sinusoidal signal with an amplitude of 0.1 radians and the frequency values f = 0.1Hz and 0.2Hz. The initial angle is set at $\theta_0 = \pi/20$ radians.

Fig. 5 visualizes the reference trajectory alongside the trajectories generated by the two comparative controllers. The external disturbance was not considered in the first simulation. Similar to the initial simulation scenario, the proposed controller exhibits faster response and superior accuracy compared to the ASMC in both values of frequency.

In the next scenario, the same external disturbance employed in the first scenario is also applied in the second simulation. As illustrated in Fig. 6, the external disturbance has minimal impact on both controllers during trajectory tracking.

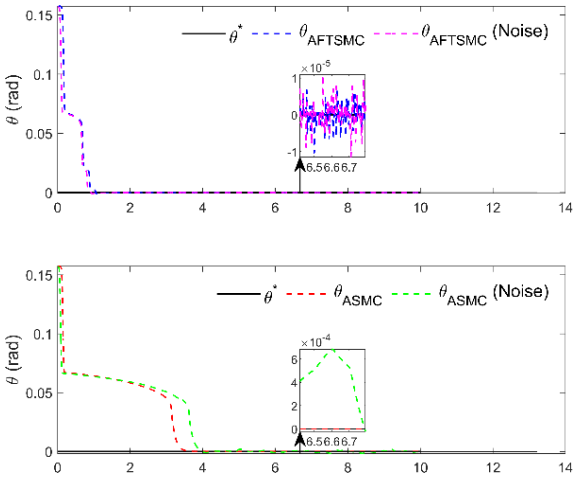

Fig. 4. The robustness of two controllers when having an external disturbance with $\theta_0 = \pi/20$.

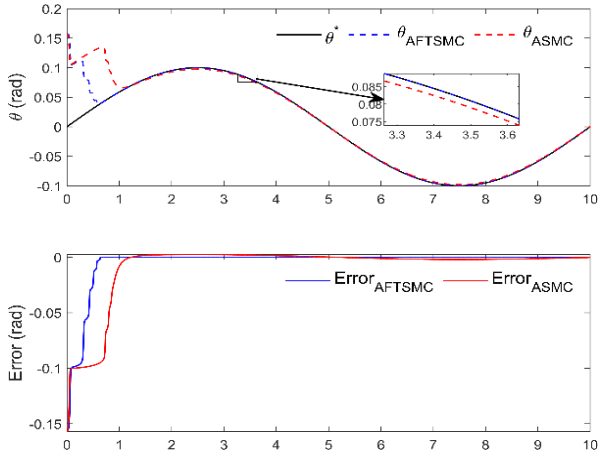

(a) f = 0.1Hz

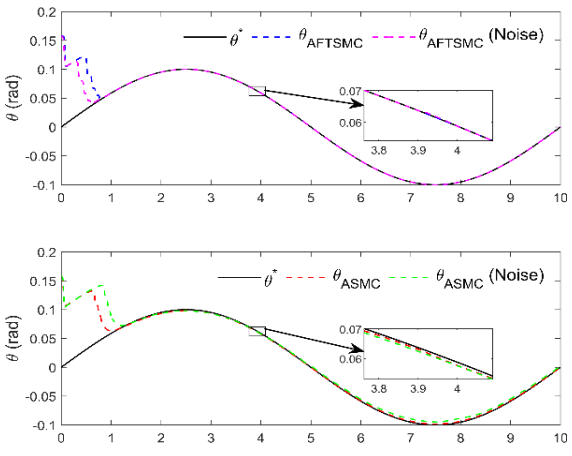

(b) f = 0.1Hz

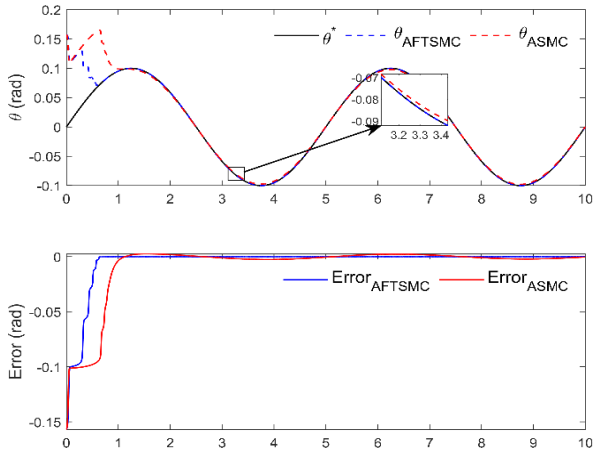

(a) f = 0.2 Hz

Fig. 5. The robustness of two controllers when tracking a sinusoidal signal without an external disturbance with (a) 0.1 Hz and (b) 0.2Hz of frequency.

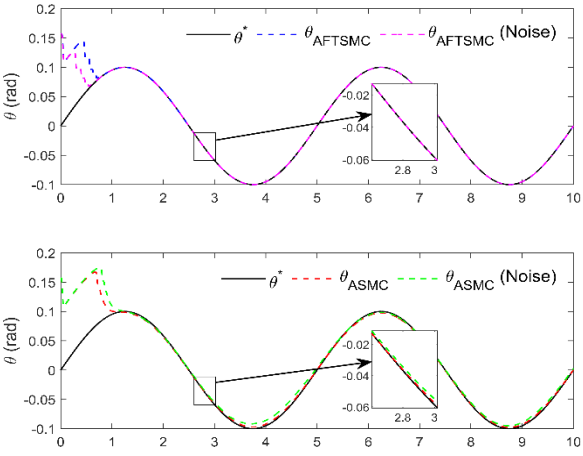

(c) f = 0.2Hz

Fig. 6. The robustness of two controllers when having an external disturbance and tracking a sinusoidal signal with (a) 0.1 Hz and (b) 0.2Hz of frequency.

5. Conclusion

In this study, we proposed and evaluated an adaptive fast terminal sliding mode control for the stabilization and trajectory tracking of an inverted pendulum on a cart. By conducting a series of simulations and comparing the results with those obtained using an adaptive sliding mode one, we thoroughly assessed the effectiveness of the AFTSMC across various scenarios.

The stability evaluation revealed that the proposed AFTSMC consistently outperformed the ASMC, demonstrating faster convergence and improved accuracy in stabilizing the pendulum under different initial conditions. Notably, when subjected to external disturbances, the AFTSMC exhibited robustness, effectively mitigating the disturbances and maintaining trajectory tracking performance.

Further assessments during sinusoidal trajectory tracking reaffirmed the superior performance of the AFTSMC. Despite the inherent challenges of inaccurate model parameters, the AFTSMC showcased resilience, proving its capability to maintain stability and trajectory tracking accuracy under these conditions.

However, it's essential to acknowledge the presence of chattering in the control signals of both controllers, as observed in the simulation results. This phenomenon highlights an area for future refinement, as excessive chattering may pose risks to actuator integrity and longevity.

In conclusion, the AFTSMC demonstrated remarkable effectiveness in stabilizing and tracking the inverted pendulum system, showcasing its robustness and resilience to external disturbances and uncertainties in model parameters. Future work may focus on addressing the chattering issue and extending the controller's applicability to real-world experimental setups, contributing to advancements in the field of nonlinear control systems.

Acknowledgments

This research was funded by Hanoi University of Science and Technology (HUST) under project number T2023-PC-036.

References

[1] J. Ferguson, A. Donaire and R. H. Middleton, Kinetic-potential energy shaping for mechanical systems with applications to tracking, IEEE Control Systems Letters, vol. 3, no. 4, pp. 960-965, Oct. 2019. https://doi.org/10.1109/LCSYS.2019.2919842

[2] José Guadalupe Romero, Alejandro Donaire, and Romeo Ortega. Robust energy shaping control of mechanical systems, Systems & Control Letters, 62(9):770-780, 2013. https://doi.org/10.1016/j.sysconle.2013.05.011

[3] Xin Xin, Seiji Tanaka, Jinhua She, and Taiga Yamasaki, New analytical results of energy-based swing-up control for the pendubot, International Journal of Non-Linear Mechanics, 52:110-118, 2013. https://doi.org/10.1016/j.ijnonlinmec.2013.02.003

[4] B. Salamat and A. M. Tonello, A swash mass pendulum with passivity-based control, IEEE Robotics and Automation Letters, vol. 6, no. 1, pp. 199-206, Jan. 2021. https://doi.org/10.1109/LRA.2020.3037861

[5] Y. Zhang, S. Li, J. Zou and A. H. Khan, A passivity-based approach for kinematic control of manipulators with constraints, IEEE Transactions on Industrial Informatics, vol. 16, no. 5, pp. 3029-3038, May 2020. https://doi.org/10.1109/TII.2019.2908442

[6] Rigatos G, Busawon K, Pomares J, Abbaszadeh M. Nonlinear optimal control for the wheeled inverted pendulum system, Robotica. 2020; 38(1): pp. 29-47. https://doi.org/10.1017/S0263574719000456

[7] E. Susanto, A. Surya Wibowo and E. Ghiffary Rachman, Fuzzy swing up control and optimal state feedback stabilization for self-erecting inverted pendulum, IEEE Access, vol. 8, pp. 6496-6504, 2020. https://doi.org/10.1109/ACCESS.2019.2963399

[8] Borase, R. P., Maghade, D. K., Sondkar, S.Y. *et al.* A review of PID control, tuning methods and applications, Int. J. Dynam. Control 9, pp. 818-827 (2021). https://doi.org/10.1007/s40435-020-00665-4

[9] Indrazno Siradjuddin, Zakiyah Amalia, Budhy Setiawan, Ferdian Ronilaya, Erfan Rohadi, Awan Setiawan, Cahya Rahmad, and Supriatna Adhisuwignjo, Stabilising a cart inverted pendulum with an augmented pid control scheme, in MATEC Web of Conferences, vol 197, pp. 11013. EDP Sciences, 2018. https://doi.org/10.1051/matecconf/201819711013

[10] S. K. Valluru, M. Singh, M. Singh and V. Khattar, Experimental validation of PID and LQR control techniques for stabilization of cart inverted pendulum system, in 2018 3rd IEEE International Conference on Recent Trends in Electronics, Information & Communication Technology (RTEICT), Bangalore, India, 2018, pp. 708-712. https://doi.org/10.1109/RTEICT42901.2018.9012643

[11] R. Banerjee, N. Dey, U. Mondal and B. Hazra, Stabilization of double link inverted pendulum using LQR, in 2018 International Conference on Current Trends towards Converging Technologies (ICCTCT), Coimbatore, India, 2018, pp. 1-6. https://doi.org/10.1109/ICCTCT.2018.8550915

[12] Sondarangallage D. A. Sanjeewa & Manukid Parnichkun Control of rotary double inverted pendulum system using LQR sliding surface based sliding mode controller, Journal of Control and Decision, 9:1, 2022, pp. 89-101 https://doi.org/10.1080/23307706.2021.1914758

[13] S. Nakatani and H. Date, Swing up control of inverted pendulum on a cart with collision by monte carlo model predictive control, in 2019 58th Annual Conference of the Society of Instrument and Control Engineers of Japan (SICE), Hiroshima, Japan, 2019, pp. 1050-1055. https://doi.org/10.23919/SICE.2019.8859912

[14] R. Firmansyah and P. P. S. Saputra, Design of model predictive control to stabilize two-stage inverted pendulum, in 2020 Third International Conference on Vocational Education and Electrical Engineering (ICVEE), Surabaya, Indonesia, 2020, pp. 1-5 https://doi.org/10.1109/ICVEE50212.2020.9243211

[15] D. Liao-McPherson, T. Skibik, J. Leung, I. Kolmanovsky and M. M. Nicotra, An analysis of closed-loop stability for linear model predictive control based on time-distributed optimization, IEEE Transactions on Automatic Control, vol. 67, no. 5, pp. 2618-2625, May 2022 https://doi.org/10.1109/TAC.2021.3086295

[16] Saqib Irfan, Adeel Mehmood, Muhammad Tayyab Razzaq, Jamshed Iqbal, Advanced sliding mode control techniques for inverted pendulum: modelling and simulation, Engineering Science and Technology, an International Journal, vol. 21, no. 4, 2018, pp. 753-759, ISSN 2215-0986. https://doi.org/10.1016/j.jestch.2018.06.010

[17] J. Huang, M. Zhang, S. Ri, C. Xiong, Z. Li and Y. Kang, High-order disturbance-observer-based sliding mode control for mobile wheeled inverted pendulum systems, IEEE Transactions on Industrial Electronics, vol. 67, no. 3, pp. 2030-2041, March 2020. https://doi.org/10.1109/TIE.2019.2903778

[18] Wang, J., Zhu, P., He, B. *et al*. An adaptive neural sliding mode control with ESO for uncertain nonlinear systems, Int. J. Control Autom. Syst, vol. 19, pp. 687-697 (2021). https://doi.org/10.1007/s12555-019-0972-x

[19] J. P. Mishra, X. Yu, M. Jalili and Y. Feng, On fast terminal sliding-mode control design for higher order systems, in IECON 2016 - 42nd Annual Conference of the IEEE Industrial Electronics Society, Florence, Italy, 2016, pp. 252-257. https://doi.org/10.1109/IECON.2016.7792972

[20] Y. Pan, C. Yang, L. Pan and H. Yu, Integral sliding mode control: performance, modification, and improvement, IEEE Transactions on Industrial Informatics, vol. 14, no. 7, pp. 3087-3096, July 2018. https://doi.org/10.1109/TII.2017.2761389

[21] Jinkun Liu and Xinhua Wang, Adaptive sliding mode control for mechanical systems, in Advanced sliding mode control for mechanical systems, 1st ed. Berlin, Heidelberg: Springer Berlin Heidelberg, 2011, pp. 117-135. https://doi.org/10.1007/978-3-642-20907-9